Aalborg Universitet

Improved Stabilization of Nonlinear DC Microgrids

Cubature Kalman Filter Approach

Kardan, Mohammad Amin; Asemani, Mohammad Hassan; Khayatiyan, Alireza ; Vafamand, Navid; Khooban, Mohammad Hassan; Dragicevic, Tomislav; Blaabjerg, Frede

Publication date:
2018

Document Version
Accepted author manuscript, peer reviewed version

[Link to publication from Aalborg University](#)

Improved Stabilization of Nonlinear DC Microgrids: Cubature Kalman Filter Approach

Mohammad Amin Kardan, Mohammad Hassan Asemani, Alireza Khayatian, Navid Vafamand, Mohammad Hassan Khooban, Tomislav Dragičević, and Frede Blaabjerg

Abstract—This paper investigates the injecting power stabilization of nonlinear DC microgrids (MGs) with constant power loads (CPLs). By considering a centralized controller scheme, the limitations of the communication utilities are considered. Therefore, limited information is transferred through the non-ideal noisy communication network. Consequently, a cubature Kalman filter (CKF) with a 3rd degree is proposed to mitigate the effect of the noisy measurement and the noisy network on the system's information. Moreover, an estimation-based robust feedback controller is developed to design an optimal value for the injecting power. The considered CKF algorithm is robust against the system uncertainty and noisy environments and has a low computational time for high-order DC MGs with a high number of sources and CPLs. In addition, a systematic procedure to compute the feedback gain of the controller is presented which can numerically be solved by linear matrix inequality (LMI) techniques. Hardware-in-the-loop (HiL) real-time simulation results verify the simplicity of the controller implementation, enhanced performance for the case of limited information, and better robustness against the noisy measurements compared to the state-of-the-art methods.

Index Terms—DC microgrid, constant power load, Cubature Kalman filter (CKF), linear matrix inequality (LMI), non-ideal communication network, hardware-in-the-loop (HiL).

I. INTRODUCTION

The advantages of the DC microgrid (MG), such as high efficiency and robustness, simple control, and natural interface for distributed generation (DG) as well as electronic loads have made it an interesting research area [1]. Among the topics, which have been studied in the DC MG, the controlling and stabilizing the DC MG with constant power loads (CPLs) have attracted a lot of attention, since the negative impedance property of the CPLs can make the overall system unstable [2], [3]. In order to alleviate undesired effects of the CPLs in such systems, several active nonlinear methods are proposed by modifying the control loop of injecting power, source converter, or load converter [4]. To stabilize the DC MGs by injecting power, several nonlinear techniques have been presented, such as backstepping controller [5], [6], sliding mode controller [7], and robust controller [8]. It should

M.A. Kardan, M.H. Asemani, and A. Khayatian are with Department of Electrical & Computer Engineering, Shiraz University, Shiraz, Iran.
N. Vafamand, M.H. Khooban. T. Dragičević, and F. Blaabjerg are with Department of Energy Technology, Aalborg University, Aalborg DK-9220, Denmark.

be noted that this study focuses on controlling the power buffer in the DC MG among other possible active methods. However, by increasing the number of CPLs, a point-to-point [9] communication from each CPL to the power buffer is not economical. Therefore, it may be preferred to control a large distributed DC MGs through a communication network [1]. Based on the way of communicating the units in the DC MGs, three general control schemes can be considered [1], including *distributed, decentralized*, and *centralized* controls. In the centralized control approach which is the basis of this paper, all information of the units collected in the control center is used and a desired reference value for the injection power is designed. Although this approach is very effective and simple, physical limitations of the communication link utilities impose critical restrictions on centralized control methods.

The communication facilities have limited bandwidth so that a limited information can be sent. Additionally, measuring all data of all units needs a high number of measurement equipment which is not economical for large DC MGs. Thereby, it is beneficial to use state estimation methods for monitoring the distributed DC MGs and performing proper stability and performance control tasks. The state estimation techniques have been attracting a lot of attention to provide a proper platform for monitoring the DC MGs, applying control and planning tasks, and improving the reliability/security of DC microgrids [10]. Because of the existing uncertainty on the DC MGs and noisy measurements and communication links, the enhanced Kalman filtering is considered as a promising solution in power electronics and power systems [10], [11]. Several applications of Kalman filters can be found in the literature, including the estimation of the rotor flux in inductor motors [12], permanent magnet flux in synchronous permanent magnet machines [13], and the state-of-charge in batteries [14], as well as reduction of the current harmonics injected to power grids [15]. In these papers, the linear Kalman filter or extended Kalman filter (EKF) are considered. However, in the case of highly nonlinear systems, tuning and implementation such filters are complicated and may exhibit divergence. The main reason is that the EKF is established based on a first-order linearization of the nonlinear dynamic system [16]. A few papers concern with employing more effective nonlinear Kalman filters. Recently in [17], an unscented Kalman filter (UKF) is employed for state estimation of the IEEE 14, 30 and 57 buses test systems with large bad data. It is illustrated that the UKF outperforms the EKF in the complex nonlinear power systems. Although the UKF does not need any iterative linearization compared to the

EKF, it still suffers the systematic error [18] and needs high computational time [19].

Cubature Kalman Filter is introduced in 2009 by Ienkaran Arasaratnam and Simon Haykin [19]. The CKF uses a spherical simplex radial rule to approximate intractable integrals while the UKF is based on an unscented transform. In the Spherical-simplex rule, intractable integrals are decomposed into two integrals: one integral on a line (radial integral) and one integral on a surface (spherical integral). The CKF has some important advantage compared with the UKF including better convergence property, filter stability, and availability of a square-root solution on the error covariance matrix [16]. In addition, the CKF uses non-product rule for sampling; meanwhile the UKF use product rules [19]. These merits motivate the usage of the CKF in practical applications.

In this paper, a novel Kalman-based output controller for stabilizing the DC MGs with CPLs, sources, and one energy storage system (ESS) is proposed. The proposed approach employs CKF, and linear matrix inequality (LMI) to design the optimal value of the power buffer. To the best knowledge of the authors, this is the first attempt to utilize the CKF in state estimation of DC MGs; meanwhile this filter has a huge performance for a wide range of nonlinear systems. In addition, by considering the exponential stability, sufficient conditions of robust linear state feedback controller are derived in terms of LMIs. The proposed approach has the following superiorities over the existing results:

1. Comparing to [10]–[14] in which the EKF is employed, the proposed approach is established based on the CKF which is more effective and does not need any Jacobian and Hessian matrices.

2. The computational time of the proposed approach is less than those consider the UKF [17].

3. The proposed controller uses the estimated states to stabilize the DC MGs, meanwhile, the approaches [5]–[8] fully utilize all of the states, which is not applicable in practice.

4. The proposed controller gain ia calculated easily by solving the newly developed LMIs.

5. The proposed LMI-based controller is merged with the CKF estimator to design the optimal value of the power buffer in the DC MGs for the first time.

Finally, to show the merits of the proposed approach several real-time simulations are carried out and the obtained results are compared with the state-of-the-art methods.

This paper is organized as follows: In Section II, the nonlinear dynamic of the DC MG is presented. In Section III, the 3rd degree CKF algorithm is studied. In Section IV, the robust linear state-feedback controller is discussed. In Section V, the simulation results are performed. Finally, the concluding remarks are given in section VI.

II. DC MICROGRID DYNAMICS

A conventional DC MG is illustrated in Fig. 1(a). This DC MG is used several applications including the electric aircraft, ships, and marine systems. As illustrated in Fig. 1(a), an AC source supplies the main bus through an AC/DC inverter.

Moreover, there exist several constant power loads (CPLs) constructed by tightly controlled converter and AC and DC loads. The simplified circuit diagram of the DC MG comprising several CPLs (systems $1, 2, \ldots, Q$), a source generator (system $Q + 1$), and a stabilizing injecting current i_{es} are shown in Fig. 1(b).
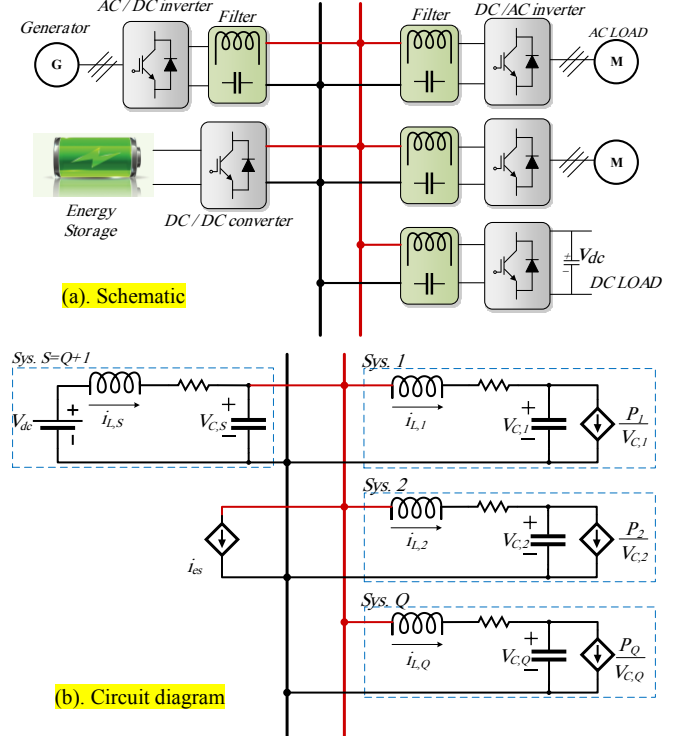

(a). Schematic

(b). Circuit diagram

Fig. 1. Detailed and simplified version of DC MG with Q CPLs.

As it is evident from Fig. 1(b), we can decouple the DC MG into $Q + 1$ subsystems with Q CPLs and one ESS. The CPLs are of the form

$$\dot{x}_j = A_j x_j + d_j h_j + A_{js} x_s \qquad (1)$$

for $j = \{1, 2, \ldots, Q\}$ and $s = Q + 1$ where $x_j = \begin{bmatrix} i_{L,j} & v_{C,j} \end{bmatrix}^T$, $i_{L,j}$ and $v_{C,j}$ are the current of the inductor and the voltage of the capacitor, respectively, in j-th CPL, and

$$A_j = \begin{bmatrix} -\dfrac{r_{L,j}}{L_j} & -\dfrac{1}{L_j} \\ \dfrac{1}{C_j} & 0 \end{bmatrix}, d_j = \begin{bmatrix} 0 \\ -\dfrac{P_j}{C_j} \end{bmatrix}, h_j = \dfrac{1}{v_{C,j}}, A_{js} = \begin{bmatrix} 0 & \dfrac{1}{L_j} \\ 0 & 0 \end{bmatrix} \qquad (2)$$

The source subsystem can be written as

$$\dot{x}_s = A_s x_s + b_s V_{dc} + b_e i_{es} + \Sigma_{j=1}^{Q} A_{cn} x_j \qquad (3)$$

where $x_s = \begin{bmatrix} i_{L,s} & v_{C,s} \end{bmatrix}^T$, $i_{L,s}$ and $v_{C,s}$ are the current of inductor and the voltage of the capacitor, respectively, in the ESS, and

$$A_s = \begin{bmatrix} -\dfrac{r_s}{L_s} & -\dfrac{1}{L_s} \\ \dfrac{1}{C_s} & 0 \end{bmatrix}, b_s = \begin{bmatrix} \dfrac{1}{L_s} \\ 0 \end{bmatrix}, A_{cn} = \begin{bmatrix} 0 & 0 \\ -\dfrac{1}{C_s} & 0 \end{bmatrix}, b_{es} = \begin{bmatrix} 0 \\ -\dfrac{1}{C_s} \end{bmatrix} \qquad (4)$$

The overall nonlinear dynamic of the DC MG is obtained by augmenting the Q CPLs and the ESS, as [20]

$$\dot{X} = AX + DH + B_{es} i_{es} + B_s V_{dc} \qquad (5)$$

where $X = \begin{bmatrix} x_1 & x_2 & \ldots x_Q & x_s \end{bmatrix}$ $H = \begin{bmatrix} h_1 & h_2 & \ldots h_Q \end{bmatrix}^T$ and

$$A = \begin{bmatrix} A_1 & 0 & \cdots & 0 & A_{1s} \\ 0 & A_2 & \cdots & 0 & A_{2s} \\ \vdots & \vdots & \ddots & \vdots & \vdots \\ 0 & 0 & \cdots & A_Q & A_{Qs} \\ A_{cn} & A_{cn} & \cdots & A_{cn} & A_s \end{bmatrix}, B_{es} = \begin{bmatrix} 0 \\ \vdots \\ 0 \\ b_{es} \end{bmatrix}, B_s = \begin{bmatrix} 0 \\ \vdots \\ 0 \\ b_s \end{bmatrix}$$

$$D = \begin{bmatrix} d_1 & 0 & \cdots & 0 \\ 0 & d_2 & \cdots & 0 \\ \vdots & \vdots & \ddots & \vdots \\ 0 & 0 & \cdots & d_Q \\ 0 & 0 & \cdots & 0 \end{bmatrix} \tag{6}$$

Applying a change-of-coordinate, the equilibrium point of the system (5) can be shifted to the origin. Let the energy storage current i_{es} be the control input, the new coordinated DC MG will be of the form [8]:

$$\dot{\tilde{X}} = A\tilde{X} + D\overline{H} + B_{es}\tilde{i}_{es} \tag{7}$$

where $\tilde{X} = [\tilde{x}_1 \ \tilde{x}_2 \ ... \tilde{x}_Q \ \tilde{x}_s] = X - X_0$, $\overline{H} = [\overline{h}_1 \ \overline{h}_2 \ ... \ \overline{h}_Q]^T$, and

$$\overline{h}_j = \frac{\tilde{v}_{C,j}}{v_{C0,j}(\tilde{v}_{C,j} + v_{C0,j})} \tag{8}$$

with X_0 is the equilibrium point of the DC MG and $v_{C0,j}$ is the equilibrium point of the $v_{c,j}$.

Fig. 2 illustrates the centralized controller scheme of the DC MG with multiple CPLs. As it can be seen from Fig. 2, each of the CPLs transfers a part of its information through a network link. Then, at the centralized controller, initially all of the system's states are estimated and a proper control law is computed. Then, the optimal value of the injecting power is sent to the ESS.
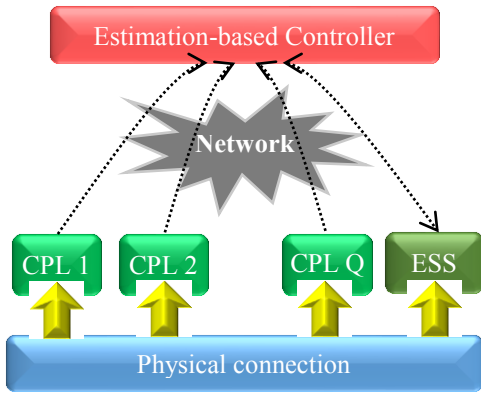

Fig. 2. Centralized controller for the DC MGs with CPLs and ESS.

The goal is to apply the online CKF algorithm to the original dynamic (5) to estimate the DC MG's states and design a simple robust controller based on (7) to assure the exponential stability of the system.

III. CUBATURE KALMAN FILTER

The CKF is a nonlinear state estimator which is highly robust against the system uncertainties, unmolded dynamics, and non-ideal noisy sensors. Moreover, the computation burden of this algorithm is low which makes this approach applicable to online state estimation of DC MGs with a high number of the CPLs. The core of the CKF is a spherical-radial cubature rule which brings about a systematic solution for nonlinear filtering issues. Consider a system with the nonlinear process and nonlinear measurement equations including additive noise in the following general form:

$$x_{k+1} = f(x_k, u_k) + w_k \tag{9}$$
$$z_k = h(x_k) + v_k \tag{10}$$

where $x_k \in \mathcal{R}^n$ is the state vector, $u_k \in \mathcal{R}^u$ is the input derived from controller, $z_k \in \mathcal{R}^m$ is the output vector, w_k is the process noise with covariance Q_k, v_k is the measurement noise with covariance R_k, $f(\cdot)$ is a nonlinear process function and $h(\cdot)$ is a nonlinear measurement function. Moreover, w_k and v_k are the uncorrelated zero-mean Gaussian white noises.

For given initial conditions and covariance error matrix, one has

$$\begin{cases} \hat{x}_{0|0} = E\{x_0\} \\ P_{0|0} = E\{(x_0 - \hat{x}_{0|0})(x_0 - \hat{x}_{0|0})^T\} \end{cases} \tag{11}$$

Then, CKF 3rd degree algorithm is as follows [19]:

Time update

1) Suppose that the current time is k. Moreover, assume that the initial mean $\hat{x}_{k|k}$ and initial covariance error $P_{k|k}$ are known. Now, first decompose $P_{k|k}$ by Cholesky decomposition as:

$$P_{k|k} = S_{k|k}S_{k|k}^T \tag{12}$$

2) In this step, cubature points are calculated by using $S_{k|k}$ and $\hat{x}_{k|k}$ as:

$$X_{i,k+1|k} = S_{k|k}\zeta_i + \hat{x}_{k|k} \quad for \ i = 1, ... 2n \tag{13}$$

3) Cubature points are expanded by the nonlinear model:

$$X_{i,k+1|k}^* = f(X_{i,k+1|k}, u_k) \tag{14}$$

4) The predicted state is estimated as follows:

$$\hat{x}_{k+1|k} = \frac{1}{2n}\Sigma_{i=1}^{2n} X_{i,k+1|k}^* \tag{15}$$

5) The predicted error is estimated as:

$$P_{k+1|k} = \frac{1}{2n}\Sigma_{i=1}^{2n}(X_{i,k+1|k}^* - \hat{x}_{k+1|k})(X_{i,k+1|k}^* - \hat{x}_{k+1|k})^T + Q_{k+1} \tag{16}$$

Measurement update

6) Covariance error is decomposed by using Cholesky decomposition:

$$P_{k+1|k} = S_{k+1|k}S_{k+1|k}^T \tag{17}$$

7) Find the Cubature points as:

$$X_{i,k+1|k} = S_{k+1|k}\zeta_i + \hat{x}_{k+1|k} \quad for \ i = 1, ... 2n \tag{18}$$

8) Expand Cubature points by using the measurement model:

$$Z_{i,k+1|k} = h(X_{i,k+1|k}, u_{k+1}) \tag{19}$$

9) Estimate the predicted measurement as:

$$\hat{z}_{k+1|k} = \frac{1}{2n}\Sigma_{i=1}^{2n} Z_{i,k+1|k} \tag{20}$$

10) Estimate the autocovariance matrix:

$$P_{zz,k+1|k} = \frac{1}{2n}\Sigma_{i=1}^{2n}(Z_{i,k+1|k} - \hat{z}_{k+1|k})(Z_{i,k+1|k} - \hat{z}_{k+1|k})^T + R_{k+1} \tag{21}$$

11) Estimate cross-covariance matrix between state variables and measurements:

$$P_{xz,k+1|k} = \frac{1}{2n}\Sigma_{i=1}^{2n}(X_{i,k+1|k} - \hat{x}_{k+1|k})(Z_{i,k+1|k} - \hat{z}_{k+1|k})^T + R_{k+1} \tag{22}$$

12) Estimate the Kalman gain as:

$$K_{k+1} = P_{xz,k+1|k} P_{zz,k+1|k}^{-1} \tag{23}$$

13) Estimate the updated state vector with the following law:

$$\hat{x}_{k+1|k+1} = \hat{x}_{k+1|k} + K_{k+1}\left(z_{k+1} - \hat{z}_{k+1|k}\right) \tag{24}$$

14) Estimate the Error Covariance by:

$$P_{k+1|k+1} = P_{k+1|k} - K_{k+1}P_{zz,k+1|k}K_{k+1}^T \tag{25}$$

Go to step (1). It should be mentioned that the above algorithm is recursive.

Remark 1 (Measurement update for linear measurement equation): If the measurement equation is linear, one can use the equations of the traditional Kalman filter in the measurement update step for simplicity. Consider the linear measurement equation and additive noise as:

$$z_k = H_k x_k + v_k \tag{26}$$

where H_k is the measurement matrix and the other variables are the same as equation (10). For a system with linear measurement equation, one can use the following measurement update equations:

$$\hat{z}_{k+1|k} = H_{k+1}\hat{x}_{k+1|k} \tag{27}$$
$$P_{zz,k+1|k} = H_{k+1}P_{k+1|k}H_{k+1}^T + R_{k+1} \tag{28}$$
$$P_{xz,k+1|k} = P_{k+1|k}H_{k+1}^T \tag{29}$$
$$K_{k+1} = P_{xz,k+1|k}P_{zz,k+1|k}^{-1} \tag{30}$$
$$\hat{x}_{k+1|k+1} = \hat{x}_{k+1|k} + K_{k+1}\left(z_{k+1} - \hat{z}_{k+1|k}\right) \tag{31}$$
$$P_{k+1|k+1} = P_{k+1|k} - K_{k+1}P_{zz,k+1|k}K_{k+1}^T \tag{32}$$

Remark 2 (Stability analysis of the CKF): When Kalman Filters are used for state estimation in a nonlinear dynamical system, stability and convergence analysis is essential. The reason is that the stability of the overall DC MG is directly dependent on the performance of the Kalman filter accuracy. Therefore, the estimation error must be zero. Stability analysis of the CKF associated with the nonlinear dynamical systems (9) and (26) with three special assumptions was previously proposed in [21], [22], in which asymptotic convergence of the estimation error system is proved by investigating a Lyapunov function.

Assumption I: The system given by (9) and (26) must be uniformly observable. To assure this assumption, the following equality must be valid [22]:

$$rank\left\| \begin{bmatrix} H_k \\ H_k \frac{\partial f}{\partial x}(x) \\ \vdots \\ H_k \left(\frac{\partial f}{\partial x}(x)\right)^{n-1} \end{bmatrix} \right\|_{x=\hat{x}_{k|k}} = n \tag{33}$$

Assumption II: The matrix $F_{k+1} = \left.\frac{\partial f}{\partial x}\right|_{x=\hat{x}_{k|k}}$ is uniformly bounded and F_{k+1}^{-1} exist.

Assumption III: The process noise covariance Q_k and instrumental matrix β_{k+1} must be chosen that

$$\bar{\sigma}[\beta_{k+1}]^2 \leq \underline{\sigma}[\beta_{k+1}]^2 \frac{\sigma[H_{k+1}]^2\underline{\sigma}[P_{k+1|k}]}{\bar{\sigma}[P_{zz,k+1|k}]} \\ + (1-\lambda)\frac{\sigma[P_{k|k}^{-1}]\underline{\sigma}[P_{k+1|k}]}{\bar{\sigma}[F_{k+1}]^2} \tag{34}$$

where $0 < \lambda < 1$, $\bar{\sigma}$ and $\underline{\sigma}$ are the maximum and minimum singular values, respectively.

In section V, it will be shown that the above assumptions are validated for the proposed CKF. Therefore, the convergence of the employing nonlinear Kalman is theoretically proved.

Remark 3 (Advantages of employing the CKF): Similar to other Kalman filters, the CKF algorithm is recursive and should be performed at each time instance. However, the computation time of the considered CKF with a 3rd degree is less than the other nonlinear Kalman filters such as particle Kalman filter, and unscented Kalman filter. Thus, the considered CKF is established based on a 3rd degree cubature rule [19]. In addition, the CKF provides a better performance and convergence than the EKF and UKF; since the cubature rule is more accurate than the unscented transformation and first/second-order linearization methods [23], [24]. Therefore, in this paper, the CKF is employed for state estimation problem of a DC MG for the first time.

IV. ROBUST STABILIZING CONTROLLER

Consider the nonlinear DC MG (7), in which the nonlinear vector $\overline{H}$ satisfies [8]

$$\overline{H}^T\overline{H} = \Sigma_{j=1}^{Q}\overline{h}_1 \leq \alpha^2\tilde{X}^TE^TE\tilde{X} \tag{35}$$

for an arbitrary scalar α and the diagonal matrix

$$E = \begin{bmatrix} E_1 & 0 & \dots & 0 \\ 0 & E_2 & \cdots & 0 \\ \vdots & \vdots & \ddots & \vdots \\ 0 & 0 & \cdots & E_Q \\ 0 & 0 & \cdots & 0 \end{bmatrix}, \quad E_i = \begin{bmatrix} 0 & 0 \\ 0 & 1 \end{bmatrix} \quad \text{for} \quad i = 1, \dots, Q \tag{36}$$

In (7), $\tilde{i}_{es}$ stands for the injecting power which stabilizes the DC MG and increases the closed-loop system robustness against the disturbances and temporary faults. To design the $\tilde{i}_{es}$, a simple linear state feedback structure of the following form is chosen

$$\tilde{i}_{es} = K\tilde{X} \tag{37}$$

where K is the feedback gain matrix and must be designed properly. To design it, an exponential Lyapunov stability theory is considered.

Definition (Exponential stability) [25]: If a Lyapunov function satisfies the inequality

$$\Gamma_4 = \dot{V} + 2\sigma V < 0 \tag{38}$$

where $\sigma \geq 0$ is the decay rate, then the Lyapunov function exponentially converges to zero and the associated closed-loop system is exponentially stable.

The closed-loop DC MG is obtained by substituting (37) into (7), as

$$\dot{X} = (A + B_{es}K)\tilde{X} + D\overline{H} \tag{39}$$

To assure the exponential stability, the following Lyapunov candidate is considered:

$$V = \tilde{X}^TP\tilde{X} \tag{40}$$

Substituting the time-derivative of (40) along the closed-loop DC MG dynamic (39) leads to

$$\dot{V} + 2\sigma V = \dot{\tilde{X}}^TP\tilde{X} + \tilde{X}^TP\dot{\tilde{X}} + 2\sigma\tilde{X}^TP\tilde{X}$$
$$= \tilde{X}^T(A + B_{es}K)^TP\tilde{X} + \overline{H}^TD^TP\tilde{X} + \tilde{X}^TP(A + B_{es}K)\tilde{X} + \tilde{X}^TPD\overline{H} + 2\sigma\tilde{X}^TP\tilde{X} \tag{41}$$

Considering the fact that $M^TN + N^TM \leq M^TM + N^TN$, yields

$$\dot{V} + 2\sigma V \leq \tilde{X}^T(A + B_{es}K)^TP\tilde{X} + \tilde{X}^TP(A + B_{es}K)\tilde{X} + 2\sigma\tilde{X}^TP\tilde{X} + \tilde{X}^TPDD^TP\tilde{X} + \overline{H}^T\overline{H} \tag{42}$$

From (35), one has

$$\dot{V} + 2\sigma V \leq \tilde{X}^T (A + B_{es}K)^T P\tilde{X} + 2\sigma \tilde{X}^T P\tilde{X} + \tilde{X}^T PDD^T P\tilde{X}$$
$$+ \alpha^2 \tilde{X}^T E^T E\tilde{X} + \tilde{X}^T P(A + B_{es}K)\tilde{X}$$
$$= \tilde{X}^T (A^T P + K^T B_{es}^T P + PA + PB_{es}K + 2\sigma P + PDD^T P \\ + \alpha^2 E^T E)\tilde{X} < 0 \quad (43)$$

By applying the Congruence lemma [25], a sufficient condition to guarantee (43) is

$$A^T P + K^T B_{es}^T P + PA + PB_{es}K + 2\sigma P + PDD^T P + \alpha^2 E^T E$$
$$< 0 \quad (44)$$

Then, application of the Schur complement [25] two times on (44), leads to

$$\begin{bmatrix} A^T P + K^T B_{es}^T P + PA + PB_{es}K + 2\sigma P & PD & E^T \\ D^T P & -I & 0 \\ E & 0 & -\alpha^{-2}I \end{bmatrix} < 0 \quad (45)$$

Pre- and post-multiplying (45) by $diag(P^{-1}, I, I)$ and its transpose, respectively and defining the variables $W = P^{-1}$, and $Z = KP^{-1}$, result in

$$\begin{bmatrix} WA^T + Z^T B_{es}^T + AW + B_{es}Z + 2\sigma W & D & WE^T \\ D^T & -I & 0 \\ EW & 0 & -\alpha^{-2}I \end{bmatrix} < 0 \quad (46)$$

In addition, the sufficient condition for satisfying $V > 0$ is

$$P^{-1} = W > 0 \quad (47)$$

Thereby, in order to design the gain matrix K of (37), one needs to solve the linear matrix inequalities (LMIs) (46) and (47) with the existing numerical solvers in the Matlab software to compute the matrices W and Z and consequently, the controller gain $K = ZW^{-1}$.

Remark 4 (Design procedure of the proposed controller): In this paper, a simple but effective linear state feedback controller is proposed for injecting a stabilizing power to the DC MGs with multiple CPLs. This approach employs the LMI technique to numerically compute controller gain matrix [26]–[28]. In other words, for a DC MG with the given system parameters, the state-space matrices A, B_{es}, and E are known. Then, by defining the LMI variables W, Z, and D, the LMI solvers compute these unknown variables such that the conditions (46) and (47) are satisfied. Finally, the controller gain is obtained by $K = ZW^{-1}$. The flowchart of the designing the controller is illustrated in Fig. 3.
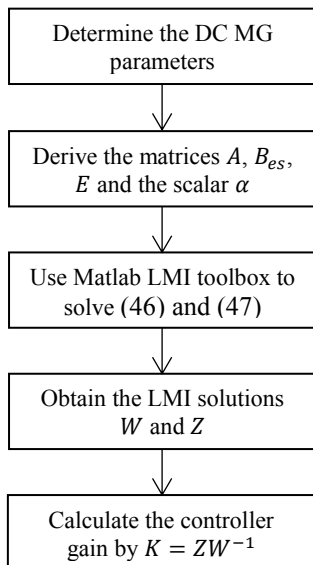

Fig. 3. The schematic of the designing the proposed controller

V. SIMULATION RESULTS

To investigate the robustness and fast transient performance of the proposed approach, it is tested on the MG with the parameters given in Table I. In addition, in order to prove the performance and robustness of the suggested approach, the hardware-in-the-loop (HiL) simulation technique is applied. One of the advantages of the real-time HiL technique in comparison to the classical off-line simulations is that it can emulate delays and errors. The layout of the HiL based on the RTS is depicted in Fig. 4. The structure of the HiL is shown in Fig. 4, which consists of 1) OPAL-RT as a real-time Simulator (RTS) which simulates the proposed controller depicted in Fig. 5; 2) a PC as the command station (programming host) in which the Matlab/Simulink based code that is executed on the OPAL-RT is generated; and 3) a router used as a connector for all the setup devices in the same sub-network. The OPAL-RT is also connected to a DK60 board [3] through Ethernet ports.

Fig. 4. The real-time simulation setup for testing the control approach.

Table I. Parameters for DC MG with two CPLs

$r_1 = 1.1\ \Omega$	$L_1 = 39.5\ mH$	$C_1 = 500\ \mu F$	$P_1 = 300\ W$
$r_2 = 0.5\ \Omega$	$L_2 = 19.5\ mH$	$C_2 = 550\ \mu F$	$P_2 = 400\ W$
$r_s = 1\ \Omega$	$L_s = 17\ mH$	$C_s = 550\ \mu F$	$V_{dc} = 200\ V$
$w_{2,1} = 130.4$	$w_{2,2} = 130.4$	$v_{C0,1} = 196.64$	$v_{C0,2} = 196.64$

For simulations, two scenarios are considered. In the first scenario, the CKF algorithm is investigated for the DC MG system without injecting the stabilizing power. Meanwhile, in the second scenario, the proposed CKF algorithm and the proposed robust controller of section IV are combined to achieve a CKF-based output feedback controller for the DC MG. Fig. 5 shows the DC MG with power and communication lines and the centralized controller to design the ESS injection power.
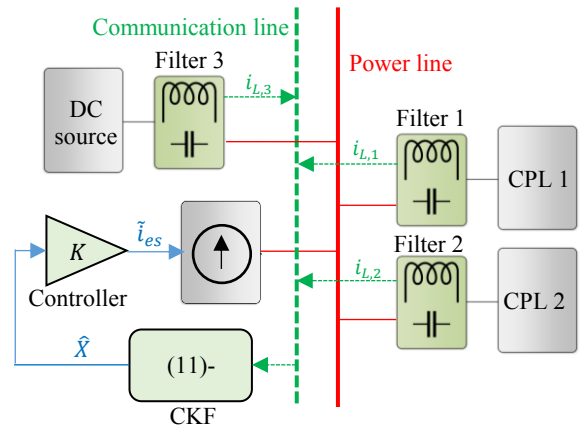

Fig. 5. The schematic of the CKF-based output feedback controller

Scenario 1: In this scenario, the effectiveness of the CKF algorithm is compared to the EKF approach which has been widely employed in the power electronics and power systems application. The parameters of the DC MG given in Table 1 are selected so that the system is stable and can converge to its equilibrium point by considering $i_{es} = 0$. For the simulation, let the initial conditions of the DC MG as $X(0) = [4.5 \ 200 \ 4.5 \ 200]^T$ and the initial condition of the Kalman filters as $\hat{X}(0) = [2 \ 100 \ 2 \ 100]^T$. Also, the variances of the system and measurement white noises for the simulation are set as $w = 0.001I$ and $v = 0.01I$, respectively. Since the system noise w is related to system uncertainties and un-modelled dynamics and in the simulations, the exact values of the system parameter are available and the DC MG is modelled precisely, a small value of system noise is chosen. In addition, the value of the measurement noise is chosen from a past experience in which the sensors measure a constant value and the noisy measures are analyzed to compute the variance of the noise. Furthermore, the initial condition of the covariance matrix as $P_0 = diag(10,10^4,10,10^4)$. The covariance matrix is selected large enough to provide a fast convergence. Fig. 6 illustrates the estimation errors of the proposed CKF and the EKF. According to this figure, one concludes that the CKF has a better performance than the EKF. In fact, the estimation errors converge to zero using the CKF after a very small transient time (about 0.02 second) without any oscillations over the time, but the estimation errors using the EKF have oscillations over the time and they don't converge to zero. Moreover, Table II is provided to demonstrate the superiority of the CKF rather than the EKF by considering Norm-2 of the state estimation errors. Table II reveals that, the Norm-2 of the state estimation errors using the CKF are much less than the ones using the EKF.

According to the assumptions of (33) in Section III, the nonlinear-linear system (9) and (26) satisfy the following equation

$$rank \begin{bmatrix} H_k \\ H_k F_{k+1} \end{bmatrix}\Bigg|_{x=\hat{x}_{k|k}} = rank \begin{bmatrix} 1 & 0 & 0 & 0 \\ 0 & 0 & 1 & 0 \\ \dfrac{-r_1}{L_1} & \dfrac{-1}{L_1} & 0 & \dfrac{1}{L_1} \\ 0 & 0 & \dfrac{-r_2}{L_2} & \dfrac{-1}{L_2} \end{bmatrix} = 4$$

Therefore, the system is uniformly observable. To check Assumption II, the matrix F should be calculated.

$$F = \begin{bmatrix} -27.85 & -25.32 & 0 & 25.32 \\ 2000 & 600000/x_2^2 & 0 & 0 \\ 0 & 0 & -25.64 & -51.28 \\ -1818.18 & 0 & 1818.18 & 0 \end{bmatrix}$$

Since, x_2 lies within a positive interval near the operating point, F is uniformly bounded and also F^{-1} exists. Thereby, Assumption II is satisfied. Moreover, by choosing the process noise covariance $Q_k = 0.001I_{4*4}$ and instrumental matrix $\beta_k = 0.001^2 I_{4*4}$, Assumption III is satisfied.
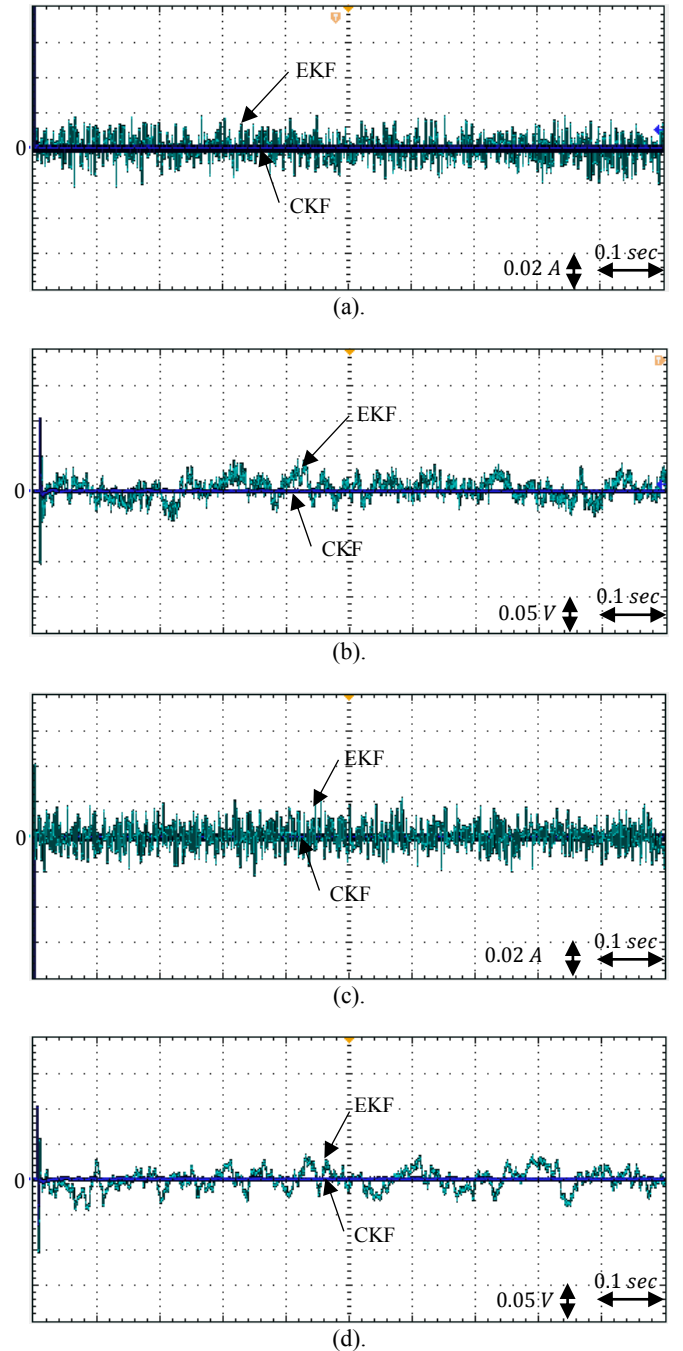

(a).

(b).

(c).

(d).

Fig. 6. Estimation error of the DC MG system. a) $e_{i_{L,1}}$, b) $e_{v_{C,1}}$, c) $e_{i_{L,2}}$, d) $e_{v_{C,2}}$.

Table II. Norm-2 of the estimation errors of the states.

	$\|e_1\|_2$	$\|e_2\|_2$	$\|e_3\|_2$	$\|e_4\|_2$
CKF	0.0469	129.2297	0.0460	103.2456
EKF	2.5220	191.7698	2.5281	140.5167

Scenario 2: In this scenario, it is assumed that the system is perturbed and the currents of voltages of the filters of the CPL and source deviate from their equilibrium point. Therefore, an injecting current is supplied to the MG to stabilize it. Thereby, the proposed robust estimated state feedback controller is merged with the CKF and the EKF in which the control law (37) uses the estimation of the system's states. In addition, to better illustrate the advantage of the state estimations in

designing the controller, an output feedback law (Output) is also considered. The output feedback controller only exploits the limited information of the DC MG; meanwhile, the EKF- and CKF-based controllers estimate all states and exploit all information of the DC MG. It is assumed that the DC MG stays in its operation point and a perturbation makes the system to go away from that point to $X(t) = [4.5\ 200\ 4.5\ 200]^T$. Fig. 7 shows the states evolutions and injecting current of the DC MG from the instant that the perturbation is occurred. As can be seen in Fig. 7, the Kalman-based control methods provide a better transient performance than the conventional output feedback controller. In order to compare further the transient performances of the controllers, Table III is added in which $t_{s,i}$ for $i = a, b, c, d$ correspond to $i_{L,1}$, $v_{C,1}$, $i_{L,2}$, and $v_{C,2}$. As can be seen from Table III, by employing the CKF-based controller, the voltage of the DC link (i.e. $v_{C,2}$) is compensated faster than the other methods.
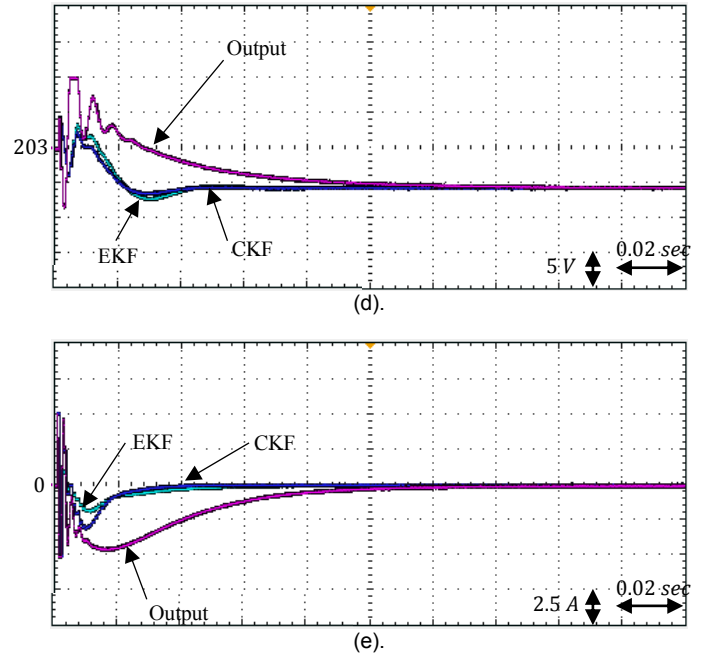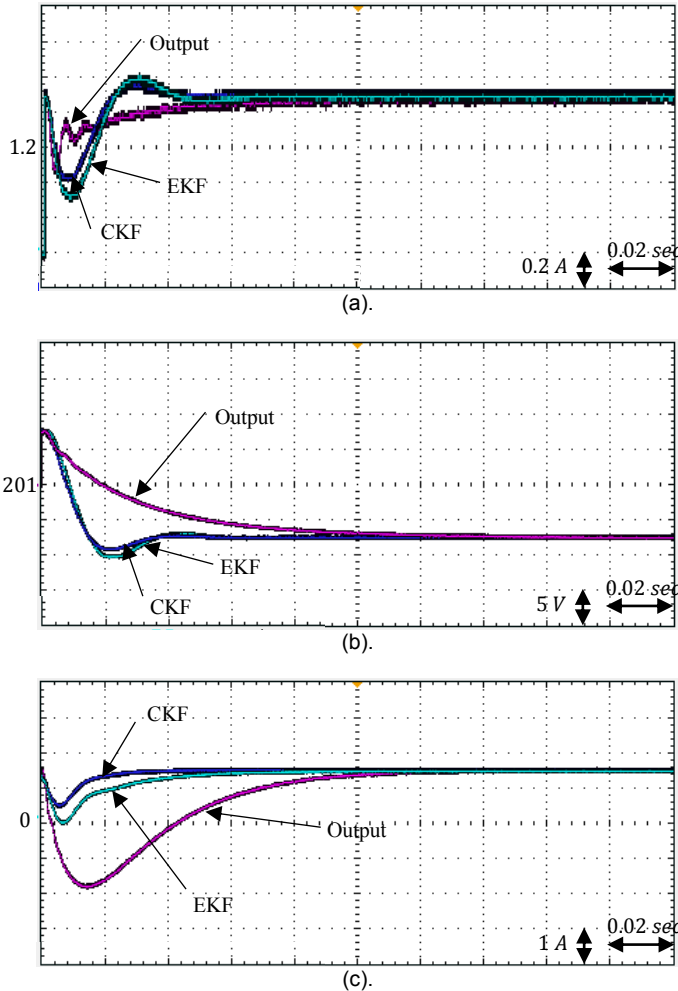

(a).

(b).

(c).

(d).

(e).

Fig. 7. States and control input evolution of the DC MG system (output feedback controller "output", EKF-based controller "EKF", and CKF-based controller "CKF"). a) $i_{L,1}$, b) $v_{C,1}$, c) $i_{L,2}$, d) $v_{C,2}$, e)i_{es}.

Table III. Settling time (2% criterion) of the system states.

	$t_{s,a}$	$t_{s,b}$	$t_{s,c}$	$t_{s,d}$
Output	44.24 ms	107.04 ms	104.85 ms	113.71 ms
EKF	44.56 ms	43.78 ms	47.44 ms	28.64 ms
CKF	44.39 ms	43.53 ms	28.29 ms	28.47 ms

I. CONCLUSION

In this paper, a novel Gaussian state estimation-based robust controller for regulating the current of the energy storage system connected to multiple CPLs in a networked DC MG is proposed. At each time instance, the CKF estimates the DC MG's states and the proper feedback law is designed based on the system's estimations. The proposed approach has a low computation time and is robust against the uncertainty and white noise. The fast estimation convergence of the CKF, as well as the exponential stability criterion, provides an output feedback controller with improved transient performance. The HiL real-time simulations verify the effectiveness and performance improvements of the proposed approach over the state-of-the-art controllers. For the future work, considering data loss in the network links and optimal selection of the CKF initial conditions can be good research topics. Also, extending the results of this paper to other topologies of DC MGs with bidirectional power flow is suggested. It should be noted that considering the droop control problem for networked DC MGs with several ESSs is of great importance.

References

[1] T. Dragicevic, X. Lu, J. Vasquez, and J. Guerrero, "DC Microgrids-Part I: A Review of Control Strategies and Stabilization Techniques," *IEEE Trans. Power Electron.*, vol. 31, no. 7, pp. 4876–4891, Jul. 2016.

[2] A. Kwasinski and C. N. Onwuchekwa, "Dynamic Behavior and Stabilization of DC Microgrids With Instantaneous Constant-Power Loads," *IEEE Trans. Power Electron.*, vol. 26, no. 3, pp. 822–834, Mar. 2011.

[3] M.-H. Khooban, T. Dragicevic, F. Blaabjerg, and M. Delimar, "Shipboard Microgrids: A Novel Approach to Load Frequency Control," *IEEE Trans. Sustain. Energy*, 2017.

[4] T. Dragicevic, "Dynamic Stabilization of DC Microgrids with Predictive Control of Point of Load Converters," *IEEE Trans. Power Electron.*, pp. 1–1, 2018.

[5] P. Magne, B. Nahid-Mobarakeh, and S. Pierfederici, "General Active Global Stabilization of Multiloads DC-Power Networks," *IEEE Trans. Power Electron.*, vol. 27, no. 4, pp. 1788–1798, Apr. 2012.

[6] Q. Xu, C. Zhang, C. Wen, and P. Wang, "A Novel Composite Nonlinear Controller for Stabilization of Constant Power Load in DC Microgrid," *IEEE Trans. Smart Grid*, pp. 1–1, 2017.

[7] M. Zhang, Y. Li, F. Liu, L. Luo, Y. Cao, and M. Shahidehpour, "Voltage Stability Analysis and Sliding-Mode Control Method for Rectifier in DC Systems With Constant Power Loads," *IEEE J. Emerg. Sel. Top. Power Electron.*, vol. 5, no. 4, pp. 1621–1630, Dec. 2017.

[8] L. Herrera, W. Zhang, and J. Wang, "Stability Analysis and Controller Design of DC Microgrids With Constant Power Loads," *IEEE Trans. Smart Grid*, vol. 8, no. 2, pp. 881–888, Mar. 2017.

[9] H. Zhang, Y. Shi, and M. Liu, "H∞ Step Tracking Control for Networked Discrete-Time Nonlinear Systems With Integral and Predictive Actions," *IEEE Trans. Ind. Inform.*, vol. 9, no. 1, pp. 337–345, Feb. 2013.

[10] Y.-F. Huang, S. Werner, J. Huang, N. Kashyap, and V. Gupta, "State Estimation in Electric Power Grids: Meeting New Challenges Presented by the Requirements of the Future Grid," *IEEE Signal Process. Mag.*, vol. 29, no. 5, pp. 33–43, Sep. 2012.

[11] F. Auger, M. Hilairet, J. M. Guerrero, E. Monmasson, T. Orlowska-Kowalska, and S. Katsura, "Industrial Applications of the Kalman Filter: A Review," *IEEE Trans. Ind. Electron.*, vol. 60, no. 12, pp. 5458–5471, Dec. 2013.

[12] M. Barut, R. Demir, E. Zerdali, and R. Inan, "Real-Time Implementation of Bi Input-Extended Kalman Filter-Based Estimator for Speed-Sensorless Control of Induction Motors," *IEEE Trans. Ind. Electron.*, vol. 59, no. 11, pp. 4197–4206, Nov. 2012.

[13] Y. Shi, K. Sun, L. Huang, and Y. Li, "Online Identification of Permanent Magnet Flux Based on Extended Kalman Filter for IPMSM Drive With Position Sensorless Control," *IEEE Trans. Ind. Electron.*, vol. 59, no. 11, pp. 4169–4178, Nov. 2012.

[14] R. Xiong, H. He, F. Sun, and K. Zhao, "Evaluation on State of Charge Estimation of Batteries With Adaptive Extended Kalman Filter by Experiment Approach," *IEEE Trans. Veh. Technol.*, vol. 62, no. 1, pp. 108–117, Jan. 2013.

[15] H. Beltrán, J. Zabalza, C. Ariño, E. Belenguer, E. Pérez, and N. Aparicio, "Improved Kalman filter based inverter control for reduction of low order current harmonics due to isolation transformers in renewable energy sources," *Renew. Energy Power Qual. J.*, vol. 1, no. 7, pp. 254–259, Apr. 2009.

[16] D. Simon, *Optimal state estimation: Kalman, H∞ and nonlinear approaches*. Hoboken, N.J: Wiley-Interscience, 2006.

[17] G. Valverde and V. Terzija, "Unscented Kalman filter for power system dynamic state estimation," *IET Gener. Transm. Distrib.*, vol. 5, no. 1, p. 29, 2011.

[18] B. Safarinejadian and N. Vafamand, "Kalman Randomized Joint UKF Algorithm for Dual Estimation of States and Parameters in a Nonlinear System," *J. Electr. Eng. Technol.*, vol. 10, no. 3, pp. 1212–1220, May 2015.

[19] I. Arasaratnam and S. Haykin, "Cubature Kalman Filters," *IEEE Trans. Autom. Control*, vol. 54, no. 6, pp. 1254–1269, Jun. 2009.

[20] N. Vafamand, M. H. Khooban, T. Dragicevic, and F. Blaabjerg, "Networked Fuzzy Predictive Control of Power Buffers for Dynamic Stabilization of DC Microgrids," *IEEE Trans. Ind. Electron.*, pp. 1–1, 2018.

[21] E. Shokri and J. Zarei, "Convergence analysis of non-linear filtering based on cubature Kalman filter," *IET Sci. Meas. Technol.*, vol. 9, no. 3, pp. 294–305, May 2015.

[22] S. Wang, W. Wang, B. Chen, and C. K. Tse, "Convergence analysis of nonlinear Kalman filters with novel innovation-based method," *Neurocomputing*, Feb. 2018.

[23] S. Wang, J. Feng, and C. K. Tse, "Spherical Simplex-Radial Cubature Kalman Filter," *IEEE Signal Process. Lett.*, vol. 21, no. 1, pp. 43–46, Jan. 2014.

[24] I. Arasaratnam, K. P. Bharani Chandra, D. Potnuru, S. B. Ch, K. Alice Mary, and D.-W. Gu, "Derivative-free square-root cubature Kalman filter for non-linear brushless DC motors," *IET Electr. Power Appl.*, vol. 10, no. 5, pp. 419–429, May 2016.

[25] K. Tanaka, *Fuzzy control systems design and analysis: a linear matrix inequality approach*. New York: Wiley, 2001.

[26] N. Vafamand and M. Sha Sadeghi, "More relaxed non-quadratic stabilization conditions for TS fuzzy control systems using LMI and GEVP," *Int. J. Control Autom. Syst.*, vol. 13, no. 4, pp. 995–1002, Aug. 2015.

[27] N. Vafamand, M. H. Asemani, and A. Khayatian, "Robust L1 Observer-based Non-PDC Controller Design for Persistent Bounded Disturbed TS Fuzzy Systems," *IEEE Trans. Fuzzy Syst.*, pp. 1–1, 2017.

[28] N. Vafamand, M. H. Asemani, A. Khayatian, M. H. Khooban, and T. Dragicevic, "TS Fuzzy Model-Based Controller Design for a Class of Nonlinear Systems Including Nonsmooth Functions," *IEEE Trans. Syst. Man Cybern. Syst.*, 2017.